RECORDSOF CHEMICAL SCIENCES

Accepted: 11th June, 2025
Published: 29th June, 2025

1. Department of Chemistry and Industrial Chemistry, Faculty of Pure and Applied Sciences, Kwara State University Malete, PMB 1530, Ilorin, Kwara State, Nigeria.

**Corresponding Author:*
Aliru Olajide Mustapha
aliru.mustapha@kwasu.edu.ng

FRsCS Vol. 4 No. 2 (2025)
Official Journal of Dept. of Chemistry, Federal University of Dutsin-Ma, Katsina State.
http://rscs.fudutsinma.edu.ng

ISSN (Online): 2705-2362
ISSN (Print): 2705-2354

Green Synthesis of Alkyd Resins from Rubber Seed Oil Functionalized with Metal Oxide Nanoparticles and Garlic Extract: Characterization and Enhanced Antibacterial Activity

**Aliru Olajide Mustapha, Saheed Olatunde Jaji, Olusola O. James, Adhiru O. Ameen*

https://doi.org/10.33003/frscs-2025-0402/05

Abstract

This study presents the synthesis, characterization, and antibacterial evaluation of bio-based alkyd resins derived from rubber seed oil. The fatty acid composition was analyzed using Fourier Transform Infrared Spectroscopy (FTIR) and Gas Chromatography–Mass Spectrometry (GC-MS), while physicochemical properties were determined following Association of Official Analytical Chemists (AOAC) standard methods. Refined rubber seed oil (RRO) showed enhanced qualities over crude oil, with iodine value (96 g I_2/100 g), acid value (0.9 mg KOH/g), saponification value (195.74 mg KOH/g), refractive index (1.48), viscosity (100), and density (0.91). Alkyd resins were synthesized via alcoholysis and polyesterification and classified into short, medium, and long oil types. Acid values decreased during polymerization, with the long oil resin having the lowest (7.60 ± 0.40 mg KOH/g), the medium oil resin achieved the highest degree of polymerization (Dp = 4.15) and functional group conversion (76%). Nanoparticles (CuO, ZnO, TiO_2) at 2% and 4% (wt/wt) were incorporated and further functionalized with garlic extract to improve antimicrobial performance. Long oil alkyd resins with hybrid nanoparticles and garlic showed the strongest antibacterial activity, with inhibition zones reaching 40.5 mm against Staphylococcus aureus. These results support the development of green, multifunctional coatings for applications in biomedical, packaging, and environmental sectors.

Keywords: Rubber seed oil, alkyd resin, nanoparticles, garlic extract, anti-bacterial

Introduction

Alkyd resins are oil-modified polyesters synthesized by the transesterification of triglyceride oils (or fatty acids), dibasic acids (or acid anhydrides), and polyols with hydroxyl functionality greater than two(] Ikhuoria et al.,2004). Due to the relatively low cost of their raw materials, alkyd resins have been widely used as binders in coatings and paint industries, and as components in industrial and household finishes (Kalu et al.,2023). The functional properties of alkyd resins, including durability and film hardness, depend strongly on the drying characteristics of the triglyceride oils utilized in their synthesis (Wagle et al.,2021; Elabor et al., 2023). Various vegetable oils such as soybean, castor, and palm oils, which contain polyunsaturated fatty acids like linoleic and linolenic acid, have been traditionally used for alkyd resin synthesis to impart flexibility, durability, and crosslinking ability to the resulting polymers (Dizman & Kaçakgil. 2023; Satheesh et al.,2010; Otabor et al.,2019; Lligadas et al.,2013). In recent years, non-conventional vegetable oils, including rubber seed oil and jatropha seed oil, have gained attention as alternative triglyceride sources for alkyd resins, offering similar properties and addressing sustainability concerns

(Elabor *et al.,* 2023; Äkräs *et al.*, 2022). Utilizing non-edible oils like rubber seed oil reduces competition with food supply chains, mitigating the global food demand challenge(Paraskar & Kulkarni, 2021; Chiplunkar *et al*., 2017). Natural rubber (*Hevea brasiliensis*) seed oil, which is abundant in Nigeria and contains approximately 45% oil classified as semi-drying, represents a promising feedstock for polymer synthesis (Flores *et al.,* 2019). Several studies have demonstrated the successful production of alkyd resins of varying chain lengths using crude rubber seed oil, attributed to its unsaturation level comparable to that of drying oils commonly used in alkyd synthesis (Aigbodion & Pillai, 2000). However, alkyd resins derived solely from rubber seed oil often face limitations such as poor alkali resistance and suboptimal drying performance, necessitating enhancement strategies (Otabor *et al*., 2019; George *et al.,* 2000).

Nanoparticle incorporation, especially metal oxide nanoparticles like titanium dioxide (TiO_2), copper oxide (CuO), and zinc oxide (ZnO), has emerged as an effective approach to improve alkyd resin properties. These nanoparticles enhance drying behavior, chemical resistance, anticorrosion effects, thermal stability, mechanical strength, and antibacterial activity in the resulting nanocomposite coatings (Sati *et al*., 2025; Ifijen *et al.,* 2022). Recent reviews emphasize the multifunctional benefits of nanoparticle-modified alkyd resins, highlighting their potential for eco-friendly, high-performance coating applications (Sati *et al*., 2025; Ifijen *et al.,* 2022).

This study aims to synthesize alkyd resins from non-edible rubber seed oil of varying oil lengths, formulate low-solvent, environmentally friendly coatings, and enhance their protective properties through the incorporation of metal oxide nanoparticles.

Materials and methods

Chemicals

All chemicals and reagents used were of analytical grade and used without further purification. Sodium hydroxide, potassium hydroxide, ethanol, chloroform, n-hexane, sodium methoxide, sulfuric acid, activated charcoal, potassium iodide, sodium sulfite, sodium chloride, glycerol, benzoic acid, lead oxide, xylene, benzene, phthalic anhydride, maleic anhydride, glacial acetic acid, acetone, dichloromethane, acetic anhydride, phenolphthalein, potassium hydrogen phthalate, petroleum ether, Wij's reagent, hydrochloric acid (HCl), ammonium hydroxide (NH_4OH), and methanol were obtained from Sigma Aldrich (UK), LGC Standards (UK), and Cerrilliant (USA).

Seeds Collection and Preparation

Three distinct non-edible seeds—crude rubber seed oil (RSO) was sourced from farms and markets in Ilorin, Kwara State, Nigeria.

Oil Extraction and Refining

Approximately 40 g of freeze-dried rubber seed was extracted with 200 mL of n-hexane under stirring at 300 rpm for 20 h at 45°C. After extraction, the solution was filtered, and the solvent was evaporated using a rotary vacuum evaporator at 40°C (Olaoluwa *et al.,* 2017). The extracted oil was stored at 4°C. Refining was conducted by degumming, neutralization with alkali,

and bleaching, following modified AOAC procedures.

$$Oil\ yield\ (\%) = \frac{mass\ of\ oil\ produced}{mass\ of\ seed\ used} \times 100 \quad (1)$$

Physicochemical characterization of the seed oil

The physicochemical properties like density, Viscosity, specific gravity, colour determination, peroxide value, odour determination, acid value, saponification value, free fatty acids and iodine value of rubber seed oil (RSO) were determined by American Oil Chemists' Society (AOCS) methods (AOAC, 1990; AOAC, 2012; Bamgboye & Adejumo, 2010)

Nanoparticle Synthesis and Garlic Functionalization

Metal oxide nanoparticles (CuO, ZnO, TiO_2) and their composites were synthesized using plantain leaf and garlic extract. Nanoparticles were added at 2 wt.% and 4 wt.% to the alkyd resin using mechanical stirring (1200 rpm) and sonication (40 kHz, 120W, 10 minutes). Garlic-enhanced nanoparticles were prepared by incorporating garlic extract into the nanoparticle suspension prior to resin blending.

Antibacterial Testing

The antibacterial performance of the resin samples was assessed following the Japanese Industrial Standard JIS Z 2801 protocol, which corresponds to ISO 22196: 2011, a standard method for evaluating antibacterial activity on non-porous surfaces. The test organisms included *Escherichia coli* (ATCC 25922), *Pseudomonas aeruginosa* (ATCC 27853), and *Staphylococcus aureus* (ATCC 25923). Bacterial suspensions were prepared in sterile saline to a 0.5 McFarland standard, equivalent to approximately 1.5×10^8 CFU/mL (Balouiri *et al.,* 2016).

Sterile nutrient agar plates were inoculated evenly with each bacterial suspension using a sterile swab. Resin-coated circular discs (10 mm diameter) were aseptically placed on the inoculated agar surfaces and incubated at 37 ± 1 °C for 24 hours under aerobic conditions. After incubation, the clear zones of inhibition surrounding each disc were measured in millimeters using a digital Vernier caliper. All tests were performed in triplicate, and the results are reported as mean values ± standard deviation to reflect reproducibility and consistency of antibacterial activity (Steinerová *et al.,* 2022; ISO 22196, 2011).

Table 1: Recipe for (short oil) the Formulation of Alkyd Resins

Ingredient (short) of RCO	Measurement
Oil/ Glycerol (g) molar ratio	1.68: 1
Phthalic anhydride / Glycerol (g) molar ratio	1.53:
Catalyst (%)	0.1
Xylene of total weight charged (%)	10
Speed (rpm)	700-800
Time (hrs)	4-5hrs

Alkyd resin preparation

The procedure for alkyd resin synthesis involved two stages: alcoholysis and esterification.

Alcoholysis stage

The oil length used for the synthesis of 200g of alkyd resins (short = 80g, medium =100g, long = 120 g), 0.01 % of CaO (catalyst) was charged into the reactor. The mixture was heated up to about 120 ºC. At 120 ºC, the amount of glycerol was added (short = 47.42 g, medium = 39.66 g, long = 31.91 g) and heated up to 230-250 ºC, maintained for 90 minutes with vigorous agitation to cause trans esterification of triglyceride into a mixture of mono- and diglyceride oils. Alcoholysis was completed when the sample of the mixture formed became soluble in 1 to 3 volumes of anhydrous methanol giving a clear solution. After this, the reaction temperature was cooled to 140°C to allow smooth introduction of the esterification stage.

Esterification stage

The temperature was lowered to 150ºC after 30 minutes, followed by the addition of phthalic anhydride (short = 72.58 g, medium = 60.34 g, long = 31.91 g), followed by the addition of xylene (10% of total weight charged) into the reaction mixture. The water of esterification evolved forms an azeotrope with xylene and is removed at intervals, after which the temperature is increased to 245ºC continuous stirring to build the molecular weight of the resin. Excess xylene was added to remove the water produced as a by-product and to increase the reaction rate. Water was thus removed with the unreacted acid by heating the bulk to a temperature above 250 ºC with continuous stirring The process of reaction, of around 150 mins was monitored by periodically checking of acid number and viscosity. The resulting solution was stopped when it was fairly viscous and the acid value was found below 10. Then, it was cooled to some extent and poured into a storage container, while still hot, for further study. The acid value of in-process samples taken at intervals was determined by titrating with a 0.1M KOH solution to the phenolphthalein end point after dissolution in a mixture of toluene and ethanol (1:1) (Bobalek & Chiang, 1964). The acid value is related to the extent of the reaction:

$$T = P_{AV} = \frac{AV_o - AV_t}{AV_O} \qquad (2)$$

Or

$$\frac{AV_t}{AV_o} = 1 - P \qquad (3)$$

The average degree of polymerization Dp as thus Eqn 4:

$$D_p = \frac{\text{no of molecules originally present}}{\text{no of molecules finally present}} \qquad (4)$$

$$\frac{AV_o}{AV_t} = (1 - P)^{-1} \qquad (5)$$

$$\frac{AV_o}{AV_t} = AV_o kt + constant \qquad (6)$$

Where AV_o is the initial acid value, AV_t is the acid value after time, t, of the reaction, k is the rate constant and t is the time of reaction (Oladipo *et al*., 2013).

Hence, a plot of AV_o/AV_t should give a straight line AVo.k from which K can be obtained. Physicochemical characterization of the synthesized Alkyd resin was carried out.

Characterization

GCMS Analysis

GC-MS analysis was carried out using Varian 3800 gas–chromatography coupled with an Agilent MS capillary column (30 m x 0.25 mm i.d). The equipment was connected to varian 4000 Mass Spectrophotometer (EI mode 70eV: m/2/ - 1000) source temperature 230 ^{O}C and quadruple temperature of 150 ^{O}C. The column temperature was initially at 200 ^{O}C (2min) and raise to 300 ^{O}C (4 min). Nitrogen (carrier) gas flow rate was set 1.0 mL/min. 1 µL volume of the oil sample was mixed with chloroform and injected using 50:1 split ratio. The mass spectrophotometer was set to scan the sample in the range of m/z 1 - 1000 with electron impact ionization mode. The samples were analyzed. A prepared pooled sample which was injected at regular intervals, was used as a control to provide a set of data for repeatability assessment. NIST Ver. 2.1 MS data library was used in the interpretation of the GC-MS chromatograms obtained. GC-MS analysis (AOAC, 2012).

FTIR Analysis

FTIR analysis was carried out using Shimadzu equipment. KBr (Potassium bromide, spectroscopy grade) was grounded into into powder form pelletized (with a hydraulic press) and scanned with the instrument as background. Then, drops of the oil sample and were mixed with KBr and pelletized using a hydraulic press, inserted into the instrument and scanned in transmittance mode at a frequency range of 4000 – 400 cm^{-1}. The method was also repeated for the synthesis of alkyd resin.

Green synthesis and modification of Alkyd resin using Metal Oxide Nanoparticles

Nanoparticles (CuO, ZnO, TiO_2) and their composites (CuO/ZnO, CuO/TiO_2, ZnO/TiO_2, CuO/ZnO/TiO_2) were synthesized using **plantain leaf extract and garlic extract** via green synthesis. The synthesized nanoparticles and their composites were dispersed into the rubber alkyd resin matrix at 2% $^{wt\%}/_{wt}$ and 4% $^{wt}/_{wt}$ using a high-shear mechanical stirrer at 1200 rpm for 30 minutes at room temperature. Uniform dispersion was ensured through sonication for 10 minutes. This formulation is referred to as NP-alkyd.

Garlic-Enhanced Nanoparticle-Modified Alkyd Resin: Garlic extract was introduced into the nanoparticle phase to enhanced its properties. These garlic-functionalized nanoparticles were then incorporated into alkyd resin following the same method above. This formulation is referred to as G-NP-alkyd.

Antimicrobial Analysis

The coating formulations' antimicrobial efficacy was tested per the JIS Z 2801 assay. The Alkyd resin was tested against both bacterial strains used were *Escherichia coli*, *Pseudomonas aeruginosa* both (Gram-negative) and *Staphylococcus aureus* (Gram-positive). These were obtained from a microbiology culture collection and maintained on nutrient agar slants. Overnight cultures were prepared in nutrient broth and adjusted to a 0.5 McFarland standard (1.5 × 10^8 CFU/mL). After incubation, the diameter of the inhibition zones (including the disc diameter) was measured in millimeters using a digital Vernier caliper. Each test was performed in triplicate, and the mean ± standard deviation was recorded (Villani *et al.*, 2020).

Results and Discussions

Physicochemical Properties of the Oils

The physicochemical properties of the oils crude rubber oil (CRO) and refined rubber oil (RRO) are presented in Table 2. The percentage oil yield of CRO is higher than RRO. The value of the density of CRO is 0.94 (g/cm^3), which is comparable to the value of 0.91 (g/cm^3) observed for RRO. The viscosity value of CRO is 130 (cp, 30 ºC), which drops to 100 (cp, 30 ºC) for RRO, reflecting the removal of high molecular weight impurities. The refractive index of the two oils remains stable, confirming minimal alterations to the oil's structure. The saponification value of CRO is 192 (mg/KOH), which increases to 195.75 (mg/KOH) for RRO as seen in Table 2, further enhances suitability for cosmetics, polymers, lubricants, and biodiesel production (Eze & Agomuo, 2021). Similarly, the iodine values for the oils were 126 and 96 g I_2/100g for CRO and RRO, respectively. The iodine value recorded in this study was also indicative of the high unsaturated fatty acid content of both oils. The iodine value is a measure of the unsaturation of triglyceride oil (Gunstone *et al.*, 1994) and is useful for predicting the drying properties of oils. The iodine value of the RRO obtained in this study was slightly lower than that recorded for CRO. The iodine values of both CRO and RRO reported in this study fall within the range of semi-drying oil, which is a potential raw material in alkyd resin (Nekhavhambe *et al*., 2019). The acid value of RRO indicates the level of free fatty acids formed from hydrolytic decomposition of glycerides to free fatty acids (Peters *et al.,* 2022) compared to RCO. High levels of free fatty acids are usually caused by age, storage conditions, and an increase in the extraction temperature of oils. The high content of free fatty acids in oils has been attributed to a reduction in oil quality (Peters *et al.,* 2022). The acid value of 3.5, obtained for CRO, was higher than a 0.9 obtained for RRO in this study. These values translate into 1.75 and 0.45 free fatty acids of RCO and RRO, respectively. The acid values obtained in this study show that both CRO and RRO are good starting materials for the production of alkyd resin, oil paints and varnishes.

Table 2. The physicochemical properties of the oils crude rubber oil (CRO) and refined rubber oil (RRO)

Physicochemical properties	**Rubber Oil (CRO)**	**Rubber Oil (RRO)**	**ASTM Standards**
Yield (%)	43	42	
Refractive Index	1.49	1.48	ASTM D1218
Density at 40ºC (g/cm^3)	0.94	0.91	ASTM D4052
Viscosity (cp, 30 ºC)	130	100	ASTM D445
Acid value, (mg/KOH)	3.5	0.9	ASTM D664
Saponification,(mg/KOH)	192	195.74	ASTM D5558
Iodine Value, (I_2/100g)	126	96	ASTM D1959
%Free Fatty Acid content (%FFA)	1.75	0.45	ASTM D1980

The refining process significantly affects several key physicochemical parameters of rubber seed oil, including its iodine value, viscosity, acid value, and FFA content, all of which are essential in determining the oil's suitability for alkyd resin production and other industrial applications. The reduction in iodine value reflects a decrease in unsaturated fatty acids, improving oxidative stability but slightly reducing drying ability. This shift is crucial for achieving the balance of properties required in high-performance coatings (Ojo & Adeyemi, 2020). The reduction in FFA content from 1.75% in CRO to 0.45% in RRO enhances the oil's oxidative stability and polymerization consistency, ensuring a more reliable and durable resin formulation (Rani & Singh, 2019). The decrease in acid value from 3.5 mg KOH/g in CRO to 0.9 mg KOH/g in RRO improves the oil's suitability for resin synthesis by minimizing unwanted side reactions during polymerization (ASTM D664).

Fatty acid composition

The fatty acid composition of the oils (CRO and RRO) is presented in Table 3. Crude rubber seed oil is primarily composed of unsaturated fatty acids, with linoleic acid ($C_{18}H_{32}O_2$) being the most abundant, constituting 37.45 %. This polyunsaturated fatty acid (PUFA) significantly contributes to the oil's drying properties, which are vital for alkyd resin production, where high unsaturation is essential for polymerization during crosslinking. Additionally, oleic acid ($C_{18}H_{34}O_2$) is another major component at 25.71%, contributing to the oil's oxidative stability and resistance to degradation. These unsaturated fatty acids impart a low viscosity and high iodine value to CRO, enhancing its suitability for industrial applications, such as paints and coatings, where drying speed is crucial. However, during refining, the content of linoleic acid decreases, which lowers the iodine value from 126 in CRO to 96 in RRO, indicating a decrease in unsaturation. This shift enhances oxidative stability but slightly reduces drying ability (Ojo & Adeyemi, 2020). Moreover, oleic acid content increases from 25.71% in CRO to 35.03% in RRO, improving oxidative stability and resistance to degradation (Emelike & Eke, 2020). This increase in oleic acid also leads to a reduction in viscosity, which makes RRO more fluid and easier to handle in industrial applications like alkyd resin synthesis.

Table 3. Fatty Acids profile of crude and refined rubber oils

Crude Rubber Oil (CRO)			**Refined Rubber Oil (RRO)**		
Composition	Saturation	Composition (%)	**Composition**	Saturation	Composition (%)
Myristic acid	**$C_{14}H_{28}O_2$**	0.16	**Caproic acid**	**$C_{14}H_{28}O_2$**	0.13
Palmitic acid	**$C_{16}H_{32}O_2$**	10.50	**Palmitic acid**	**$C_{16}H_{32}O_2$**	8.93
Palmitoleic acid	**$C_{16}H_{30}O_2$**	0.20	**Palmitoleic acid**	**$C_{16}H_{30}O_2$**	0.09
Stearic acid	**$C_{18}H_{36}O_2$**	10.25	**Heptadecanoic acid**	**$C_{17}H_{34}O_2$**	0.09
Oleic acid	**$C_{18}H_{34}O_2$**	25.71			
Linoleic acid	**$C_{18}H_{32}O_2$**	37.45	**Stearic acid**	**$C_{18}H_{36}O_2$**	3.80
Arachidic acid	**$C_{20}H_{40}O_2$**	0.44	**Oleic acid**	**$C_{18}H_{34}O_2$**	16.52
Linolenic acid	**$C_{18}H_{30}O_2$**	14.68	**Linoleic acid**	**$C_{18}H_{32}O_2$**	59.21
cis-11-Eicosenoic acid	**$C_{20}H_{38}O_2$**	0.60	**Arachidic acid**	**$C_{20}H_{40}O_2$**	0.16
			Linolenic acid	**$C_{18}H_{30}O_2$**	9.93
			cis-11-Eicosenoic acid	**$C_{20}H_{38}O_2$**	0.30
				$C_{22}H_{40}O_2$	0.47
			cis-13,16-Docosadienoic acid	**$C_{24}H_{48}O_2$**	0.37
			Lignoceric acid		
% Saturation		21.35		13.48	
% Unsaturation		78.64	% Saturation	86.52	
			% Unsaturation		

The decrease in polyunsaturated fatty acids (PUFAs) like linolenic acid ($C_{18}H_{30}O_2$), which drops from 14.68% in CRO to 2.56% in RRO, also plays a significant role in the oil's suitability for alkyd resin synthesis. Linolenic acid contributes to the drying properties of the oil, but excessive amounts can compromise oxidative stability, leading to faster degradation. The reduction in linolenic acid during refining improves the oil's oxidative stability while sacrificing some drying properties. (Rani & Singh, 2019).

FT-IR analysis of the Rubber Oils.

Castor oil – FTIR (KBr, cm^{-1}): -O-H (3371 cm^{-1}), C-H (2927 & 2857 cm^{-1}), -COO- (2357 cm^{-1}), C=C (1593 cm^{-1}), C-H bending (1365 cm^{-1}) and –C-O (1035 cm^{-1}).

FTIR study of rubber oil, which supports the presence of unsaturated acyl groups in the oils presented in Figure 1. The results show that the functional groups present in RRO are similar to those in other vegetable oils Oladipo *et al.,* (2013). Since the oil is composed of essential fatty acids and esters it was observed that its FT-IR spectra were

found at similar frequencies of absorption; the O-H carboxylic acid stretch which was observed at the 3371 $cm^{-1.}$ The characteristic absorption frequency observed between 2927 and 2857cm-1 of the oils showed C-H stretching vibration of the olefinic functional group, and the stretching frequency of alkene C=C was observed at approximately 1593 cm^{-1} (Okieimen *et al*., 2005).

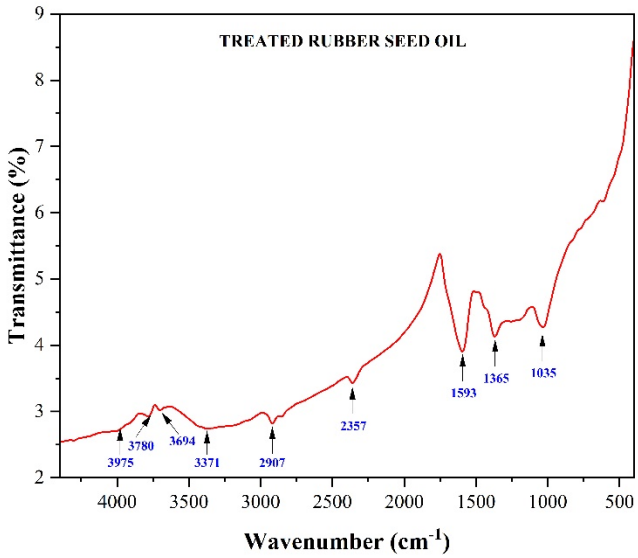

Figure 1. FTIR result of refined rubber oil

The C=O stretching of carboxylic and triglycerides (ester) was observed at 664 cm^{-1} in the oil. The level of unsaturation as well as the iodine value of vegetable oil have been determined using the ratios of intensities of the observed (νC=C) bands at 1650 cm^{-1}, as well as ν=C-H at 3010 cm^{-1} and 2853 cm^{-1}, which are well reported in the literature Mohammadi *et al.,*(2023). The physicochemical characteristics of rubber oil obtained in this study are similar and comparable to those of the seed oils currently used in the commercial production of alkyd resins (Rozali *et al*., 2023).

Properties of Rubber-Based Alkyd Resins

The synthesis of alkyd resins from rubber oil involves several key parameters that can be used to assess the success of the reaction and the properties of the resulting resin. The acid values, reaction time and the percentage conversion of functional groups (%P) for the finished alkyds were monitored using these values to ensure complete reaction with a corresponding higher degree of polymerization (Dp), as presented in Table 4.

Acid Value

The acid values of the synthesized Rubber-based resins ranged from 35.91± **0.45** to 9.46± **0.40** mgKOH/g, for short rubber, 34.75 ± 0.52 to 8.37 ± 0.51 mg KOH/g for medium rubber and 25.70 ± 0.68 to 7.60 ± 0.40 mg KOH/g for long rubber alkyd. The acid values of all the rubber alkyd-resin show a clear decrease as the time of reaction proceeds from $T_{0.0}$ to T_{120}, reflecting the progressive conversion of free fatty acids into esterified products. This

reduction aligns with the observations of (Adeosun & Oladipo, 2014) and agrees with reaction time increased, signaling sucess the findings of (Mustapha *et al.,* 2023) who also reported a decrease in acid value as the polymerization as presented in Figure 2.

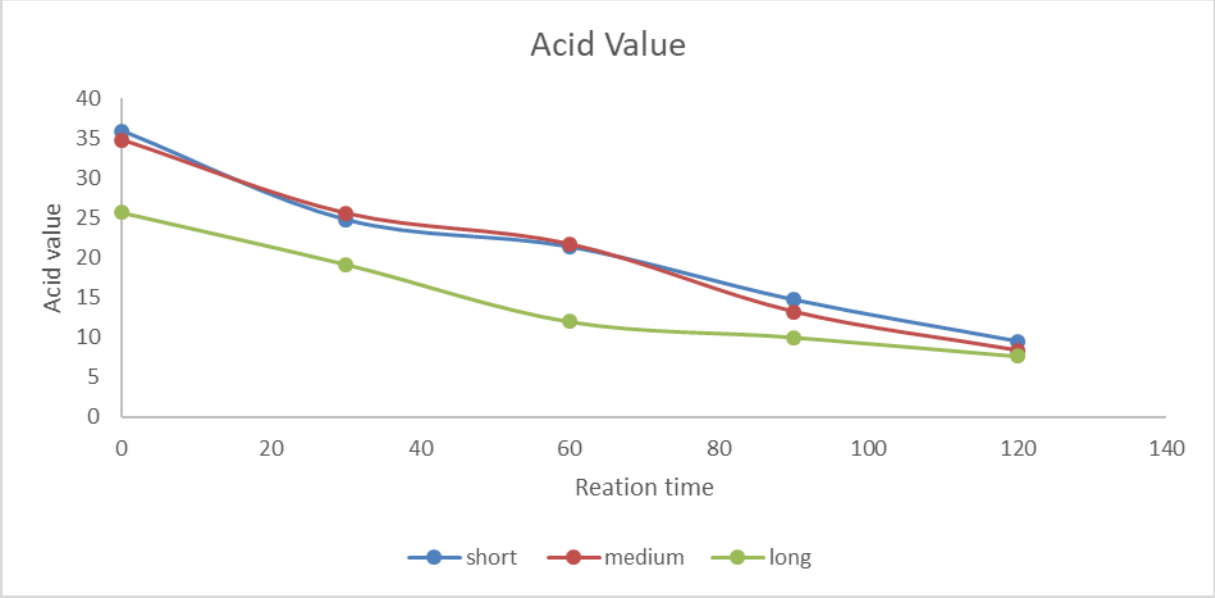

Figure 2. Acid Value of rubber alkyd resin

Degree of polymerization (Dp)

The degree of polymerization (Dp) is an indicator of the extent of polymer chain formation in the resin, reflecting the molecular weight and structural complexity of the alkyd resin as presented in Table 4. Dp increased from 0 to 3.80, 4.15 and 3.38 for short, medium and long rubber alkyd resin, respectively, as the time of reaction proceeded from T_0 to T_{120}. This rise in Dp is typical of alkyd resin synthesis, , resulting in resins with enhanced mechanical and thermal properties (Menkiti & Onukwuli, 2011). Similar trends were observed in the report of (MacDonald & McKeen, 1994), which highlighted the importance of reaction time in controlling polymerization of the resin as presented in Figure 3.

Functional group percentage conversion (%P)

The percentage conversion (%P) of functional groups provides a quantitative measure of the overall extent of the esterification reaction, as presented in Table 4, the % P of the increased from 0 % to 73 %, 76% and 70% for short, medium and long rubber based-alkyd resin respectively, as the reaction time increase from T_0 toT_{120}, these data indicate that as the reaction time increases, a greater proportion of the rubber seed oil is converted into alkyd resin. This aligns with findings by (Uzoh *et al.,* 2016), who reported similar trends in functional group conversion during the synthesis of alkyd resins from rubber seed oil**.** This upward trend highlights the growing incorporation of the oil's fatty acids into the resin structure, facilitating the formation of a more complete polymer network as presented in Figure 4.

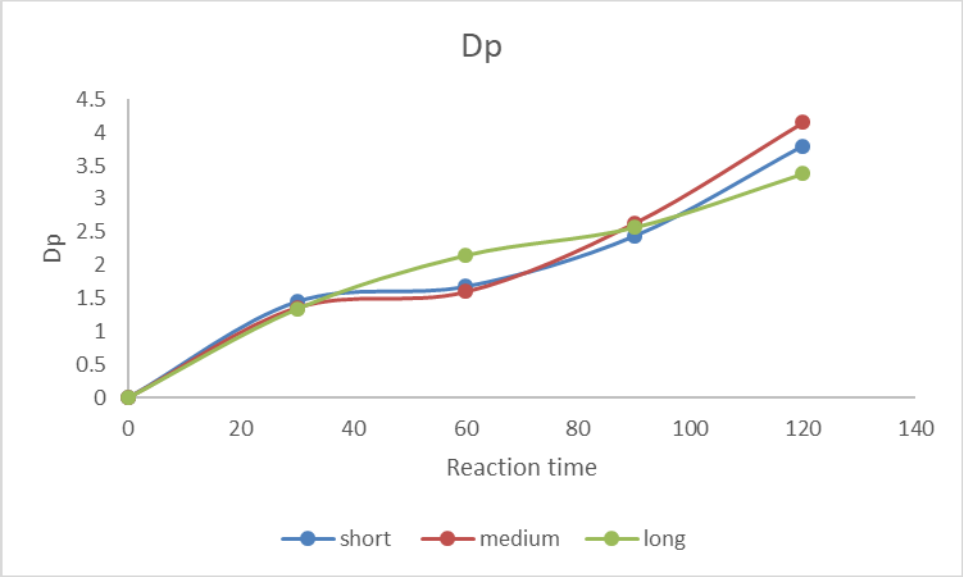

Figure 3: Degree of polymerization (Dp) of rubber alkyd resin

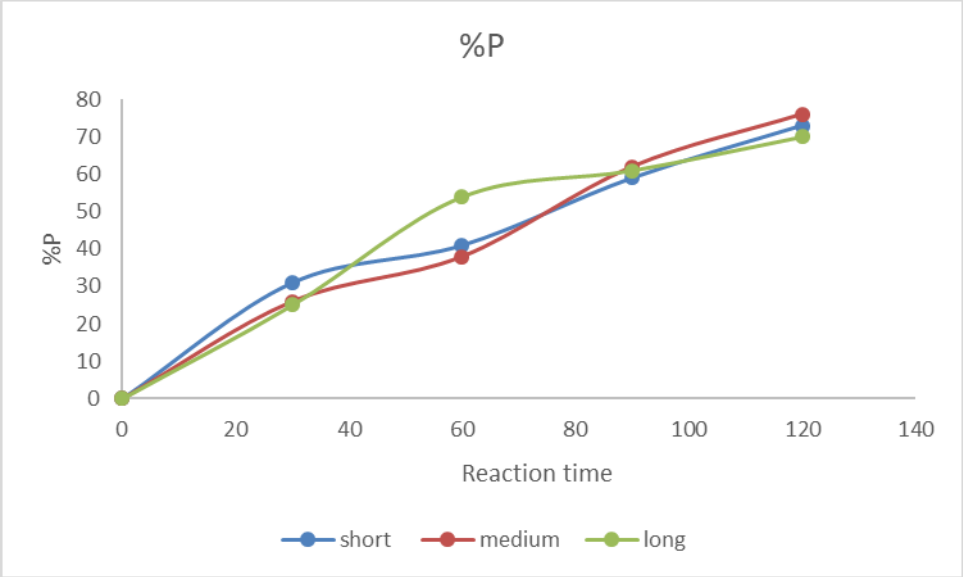

Figure 4. Percentage conversion (%P) of rubber alkyd resin

Table 5: Acid value of rubber-based-alkyd resin

S/N	Reaction time	Short			Medium			Long		
		Acid value	Dp	%P	Acid value	Dp	% P	Acid value	Dp	%P
1	$T_{0.0}$	35.91±0.45	-	-	34.75±0.52	-	-	25.70±0.65	-	-
2	T_{30}	24.75±0.11	1.45	31	25.56±0.88	1.36	26	19.18±0.92	1.34	25
3	T_{60}	21.34±0.16	1.68	41	21.7±0.28	1.60	38	11.96±0.71	2.15	54
4	T_{90}	14.69±0.48	2.44	59	13.22±0.49	2.63	62	9.99±0.96	2.57	61
5	T_{120}	9.46±0.40	3.80	73	8.37±0.51	4.15	76	7.60±0.40	3.38	70

(Dp) degree of polymerization, (P) conversion of functional groups, (%P) percentage conversion of functional groups.

The characterization data of alkyd resins synthesized from long rubber seed oil reveal that reaction time plays a critical role in the resin's physicochemical properties. The significant reduction in acid value, increase in degree of polymerization, and rise in functional group percentage conversion over time confirm that prolonged reaction times lead to more efficient esterification and improved resin quality. These findings are consistent with established literature (Ibrahim & Al-Sabagh, 2020), and suggest that long rubber seed oil is a promising feedstock for the production of high-performance, eco-friendly alkyd resins suitable for industrial applications.

GC-MS Analysis

The GC-MS analysis of rubber alkyd resin reveals a diverse range of chemical constituents, offering insights into the resin's structural composition and its potential industrial applications. Among the most prominent compounds in the short rubber alkyd resin were phthalic anhydride (9.53 %), oleic acid (19.12 %), and 9-octadecenoic acid (Z)-, methyl ester (7.35 %) as presented in Figure 5. The following fatty acids were identified in the medium resin, which include n-hexadecanoic acid (5.70 %), hexadecanoic acid, methyl ester (3.56 %), 9-octadecenoic acid (Z)-, methyl ester (7.87 %), and 9-octadecenoic acid (E) (34.60 %) as presented in Figure 6. These compounds are integral to the resin's drying properties, oxidative stability, and flexibility. Specifically, 9-octadecenoic acid (E), which dominates the profile with 34.60 %, is a monounsaturated fatty acid that contributes to the resin's ability to undergo oxidative curing, a key feature of alkyd resins used in coatings, While for long rubber-alkyd resin, the predominant compounds identified in the long rubber alkyd resin include linoelaidic acid (15.85% and 11.41 %), 9,17-octadecadienal (Z) (14.66 % and 18.72 %), 1H-indene, 2-butyl-5-hexyloctahydro (18.68 %), and octadecanoic acid, 2,3-dihydroxypropyl ester (12.60 %), as presented in Figure 7. The presence of these compounds aligns with findings by (Patel & Desai, 2020), who demonstrated that unsaturated fatty acids and their derivatives significantly contribute to the polymerization and oxidative curing processes in alkyd resins. The significance of this compound in alkyd resins has been

corroborated by (Patel & Desai, 2020), who noted that such fatty acids enhance polymerization and curing efficiency, improving the resin's overall durability and resistance to cracking.

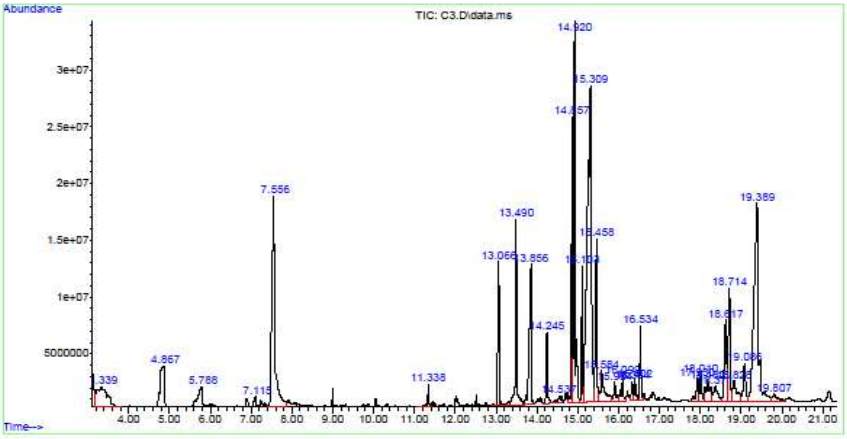

Figure 5: GC-MS chromatogram of Rubber Alkyd Resin Short

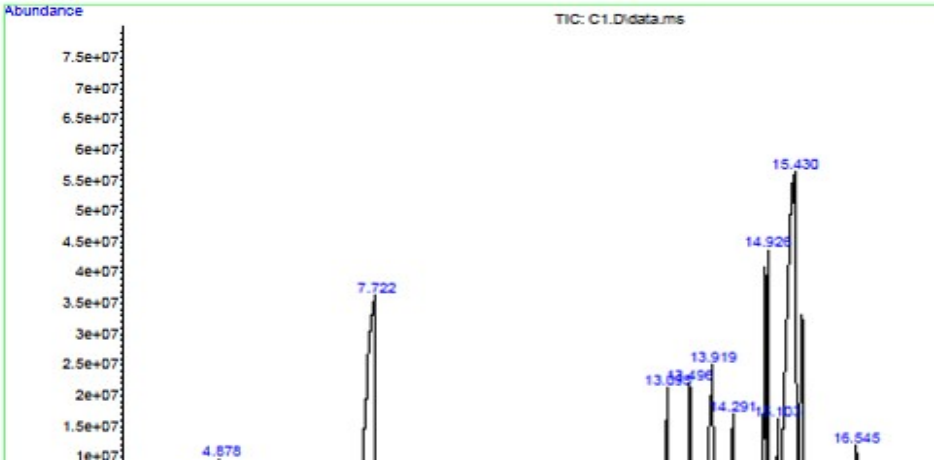

Figure 6: GC-MS chromatogram of Rubber Alkyd Resin Medium

Figure 7: GC-MS chromatogram of Rubber Alkyd Resin Long

FTIR Analysis of Rubber Alkyd Resins

The FT-IR spectra of the short, medium and long alkyd resins are presented in Figure 8. The major functional groups are listed in below.

Short-FTIR (KBr, cm^{-1}): -O-H (3418 cm^{-1}), C-H (2920 cm^{-1}), -COO- (2339 cm^{-1}), C=C (1623 cm^{-1}), -C-O (1105 cm^{-1}).

Medium-FTIR (KBr, cm^{-1}): -O-H (3418 cm^{-1}), C-H (2884 cm^{-1}), -COO- (2359 cm^{-1}), C=C (1626 cm^{-1}), -C-O bending (1307 cm^{-1}) and –C-O-C (1028 cm^{-1}).

Long-FTIR (KBr, cm^{-1}): -O-H (3418 cm^{-1}), C-H (2933 cm^{-1}), -COO- (2368 cm^{-1}), C=C (1627 cm^{-1}), -C-O (1070 cm^{-1}).

The IR spectra of the short, medium & long rubber-based alkyd resins were identical and similar in all aspects. Consequently, the spectra support the presence of ester, aromatic, and hydroxyl groups and olefinic double bonds in the alkyd resins. The strong absorption bands at 2339 cm^{-1}, 2359 cm^{-1} & 2368 cm^{-1} for short, medium and long respectively, show a characteristic of the stretching frequency of the carbonyl group of the alkyd resins. A sharp absorption peak appears at 1623 cm^{-1}, 1626 cm^{-1} & 1627 cm^{-1} for short, medium and long respectively, which are characteristic of the unsaturation group on the alkyd resin backbone. The broad-band at 3418 cm^{-1} present in all the alkyd resins confirms the presence of -OH groups and is characteristic of alkyd resins (Elabor *et al*., 2023). A strong absorption due to the symmetrical -C-O-C stretching band at 1105 cm^{-1}, 1028 cm^{-1} & 1070 cm^{-1} for short, medium and long, respectively. These peaks are attributed to the stretching of the ether group, which were also observed (Elabor *et al.,* 2023; Chiplunkar & Pratap, 2016).

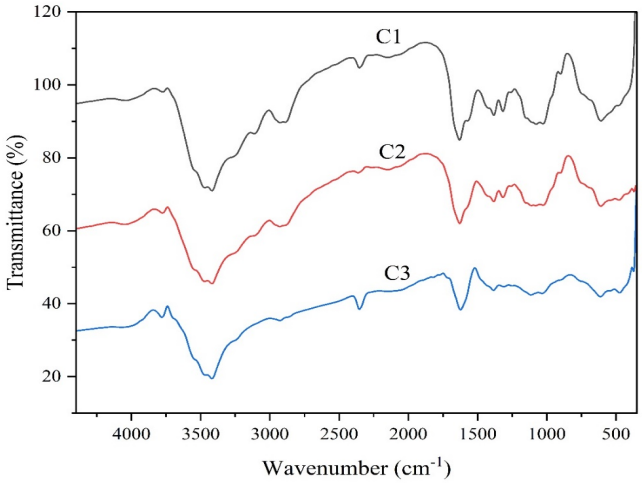

Figure 8: FTIR Comparative spectra of different Rubber Oils Alkyd resin

Antibacterial Analysis

The antibacterial potential of the prepared rubber alkyd resin-based modified with garlic extracts and (CuO, ZnO,TiO_2) and their composites were assessed using the zone of inhibition (ZOI) assay, against *Staphylococcus aureus, Escherichia coli* and *Pseudomonas aeruginosa* with susceptibility thresholds defined as resistant (≤10 mm), intermediate (10–20 mm), and susceptible (≥20 mm) as present in Table 6 and Table 7 and Fig 9 and Figure 10.

***Escherichia coli* ATCC 9637**

Test isolate shows**:** Short-oil resin performed best (20 mm), while medium and long-oil resins showed similar, lower activities (15 mm). CuO and ZnO nanoparticles modified with garlic extract in short-rubber alkyd resin showed notable antibacterial effects, with inhibition zones of 38 ± 9.90 mm and 31 ± 12.73 mm, respectively. The ZnO/TiO_2 nanocomposite in medium resin displayed the highest inhibition zone (31 ± 12.73 mm), suggesting enhanced efficacy through the combined action of ZnO and TiO_2 nanoparticles, synergistically amplified by garlic. This supports previous findings on the antimicrobial efficacy of garlic-modified nanoparticles (Kumar & Kumar, 2019). In the long-oil rubber resin, the CuO/ZnO/TiO_2 composite produced a zone of inhibition of 38 ± 2.83 mm, again underscoring the synergistic role of the three nanoparticles combined with garlic extract.

***P. aeruginosa* ATCC 10145**

Test isolate: Long oil resin exhibited the highest inhibition (17.5 mm), Medium oil was moderate (15 mm) and Short oil had the lowest (12.5 mm). ZnO modified with garlic extract in short-rubber alkyd resin showed the highest susceptibility with a ZOI of 20 ± 2.73 mm, classifying it as susceptible (S). CuO and CuO/ZnO, showed intermediate activity with ZOIs of 17.5 ± 1.73 mm and 17.5 ± 11.73 mm, respectively and TiO_2 and its composites demonstrated limited activity, with TiO_2 alone being resistant (12.5 ± 11.53 mm). for medium rubber alkyd resin, CuO exhibited strong antibacterial activity with a ZOI of 30 ± 2.30 mm, CuO/TiO_2 composite demonstrated susceptibility (29.5 ± 1.73 mm). ZnO and CuO/ZnO showed intermediate activity. Furthermore, for long alkyd resin, all tested nanoparticles & composites were either resistant or intermediate, with no ZOI surpassing the 20 mm threshold.

***Staphylococcus aureus* ATCC 13709**

Test isolate: The medium-oil alkyd resin showed the highest antibacterial activity (30 mm), followed by the short-oil (17.5 mm) and long-oil resin (15 mm). The CuO/ZnO composite modified with garlic extract in the short-oil resin demonstrated the highest ZOI (37.5 ± 17.68 mm), indicating strong synergistic activity. Other composites, such as CuO/TiO_2 (32.5 ± 3.54 mm) and ZnO/TiO_2 (29 ± 4.24 mm), also exhibited strong antibacterial effects. In medium-oil resin, CuO and ZnO individually produced high ZOIs (37 ± 32.53 mm and 37 ± 25.46 mm, respectively), though they displayed very large standard deviations, indicating inconsistency among replicates. These variations suggest formulation or dispersion-related variability, possibly due to incomplete nanoparticle homogenization,

agglomeration, or differences in resin viscosity during mixing and curing. In long-oil resin, the CuO/ZnO/TiO_2 composite maintained strong activity (34 ± 14.14 mm), further emphasizing its potential. ZnO/TiO_2 also showed good efficacy (34.5 ± 0.71 mm).

It is important to note that several formulations exhibited high standard deviations—for example, the CuO/ZnO composite in *S. aureus* tests (37.5 ± 17.68 mm), and ZnO in medium-oil resins (37 ± 25.46 mm). These values indicate poor reproducibility and potential intra-sample heterogeneity. Such variability may arise from uneven dispersion of nanoparticles within the alkyd matrix, inadequate mixing, or aggregation of garlic-modified nanomaterials, which can affect uniformity and antimicrobial release profiles.

All antibacterial tests were performed in triplicate (n = 3), and the results are presented as mean ± standard deviation. Although clear trends were observed, future work should incorporate statistical analysis to validate observed differences and quantify significance. Furthermore, graphical data should include error bars, and cases of high variability should be explicitly discussed to aid interpretation.

Mechanistic gaps: The enhanced antibacterial activity of CuO/ZnO combinations compared to TiO_2 alone may be attributed to synergistic ROS generation and ion-mediated membrane disruption. Cu^{2+} and Zn^{2+} ions are known to penetrate bacterial membranes, inhibit enzymes, and induce oxidative damage, whereas TiO_2 primarily exhibits photocatalytic effects, which are limited in the absence of UV activation (Rajendran *et al*., 2021).

Conclusion

In conclusion, this study developed bio-based antimicrobial alkyd resins from rubber seed oil. The results showed that refined rubber seed oil (RRO) improved the physicochemical properties and performance characteristics of the finished alkyd resins compared to crude rubber seed oil (CRO). Medium rubber alkyd resin, with an acid value of 8.37 and a percentage polymerization of 76%, demonstrated solid polymerization efficiency and a strong balance between reactivity and stability. The long rubber seed oil-based alkyd resin exhibited notable antibacterial activity, particularly with CuO/ZnO and ZnO nanoparticles; however, antibacterial efficacy varied among bacterial strains, with some resistance observed in *Pseudomonas aeruginosa* in the long alkyd resin. FTIR and GC-MS analyses confirmed the chemical structure and functional groups of the resins, supporting the suitability of rubber seed oil as a promising raw material for the coatings industry. It is important to note some limitations, including possible nanoparticle aggregation and potential long-term stability issues, which may affect sustained antibacterial performance and require further investigation. This work contributes to expanding the value of non-conventional rubber seed oil, potentially benefiting agricultural and rural development through increased demand.

Table 6: Antibacterial activities of alkyd resins against test isolate.

Akyld resin	(zone diameter of inhibition in mm)			
		S. aureus	***E. coli***	***P. aeruginosa***
Rubber	Short	17.5	20	12.5
	Medium	30	15	15
	Long	15	15	17.5

Interpretation: *Susceptible (≥ 20 mm zone of inhibition), Intermediate (≥10-20 mm zone of inhibition), Resistant: (≤ 10 mm zone of inhibition).*

Table 7: Antibacterial activities of rubber oil-alkyd resin with metal oxide nanoparticles modified with garlic extract against *E. coli, P. aeruginosa and Staphylococcus aureus*

Bacterial agent	**Extracts at 100mg/ml (zone diameter of inhibition in mm)**							
		CuO	**ZnO**	**TiO_2**	**CuO/TiO_2**	**ZnO/TiO_2**	**CuO/ZnO**	**$CuO/ZnO/TiO_2$**
Escherichia coli	Short	38±9.90	R	21.5±9.19	20.5±13.44	20.5±0.71	31.5±28.99	27.5±4.95
	Medium	18±0.00	R	26±1.41	27.5±10.61	R	22±15.56	20±7.07
	Long	32.5±24.75	34±7.07	16.5±2.12	30±0.00	26.5±23.33	19.5±6.36	38±2.83
Pseudomonas aeruginosa	Short	17.5±1.73	20±2.73	12.5±11.53	15±12.73	R	17.5±11.73	14.5±1.73
	Medium	30±2.30	15±4.13	15±12.24	29.5±1.73	15±1.73	22.5±13.73	20±3.73
	Long	15±11.7	15±1.23	17.5±2.58	R	15±2.73	17.5±1.73	15±2.73
Staphylococcus aureus	Short	21±12.73	17.5±0.71	27.5±10.61	32.5±3.54	29±4.24	37.5±17.68	21.5±4.95
	Medium	37±32.53	37±25.46	23±11.31	18.5±9.19	15.5±0.71	22.5±3.54	20±7.07
	Long	40±7.07	30±7.07	26.5±2.12	32.5±10.61	34.5±0.71	37.5±3.54	34±14.14

Susceptible (≥ 20 mm zone of inhibition), Intermediate (≥10-20 mm zone of inhibition), R= Resistant: (≤ 10 mm zone of inhibition).

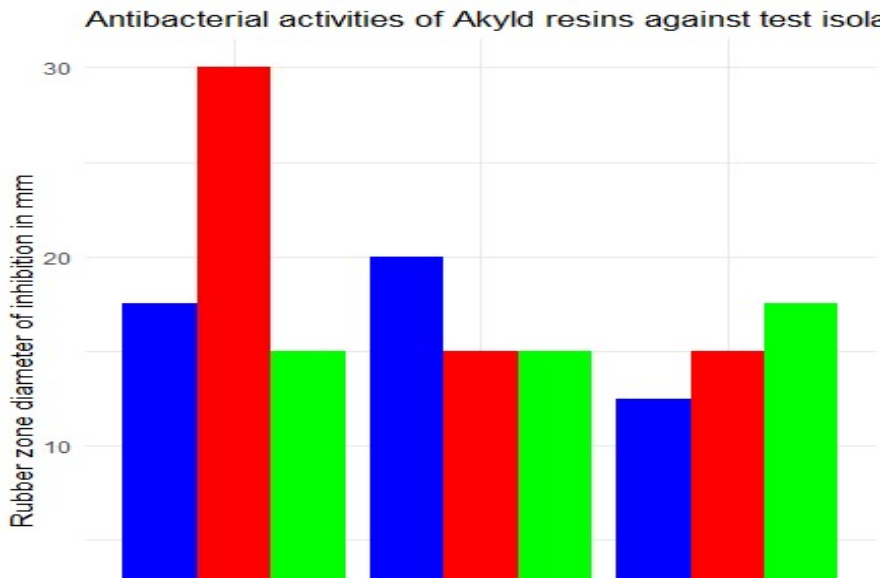

Figure 9: Antibacterial activities of alkyd resins against the test isolate

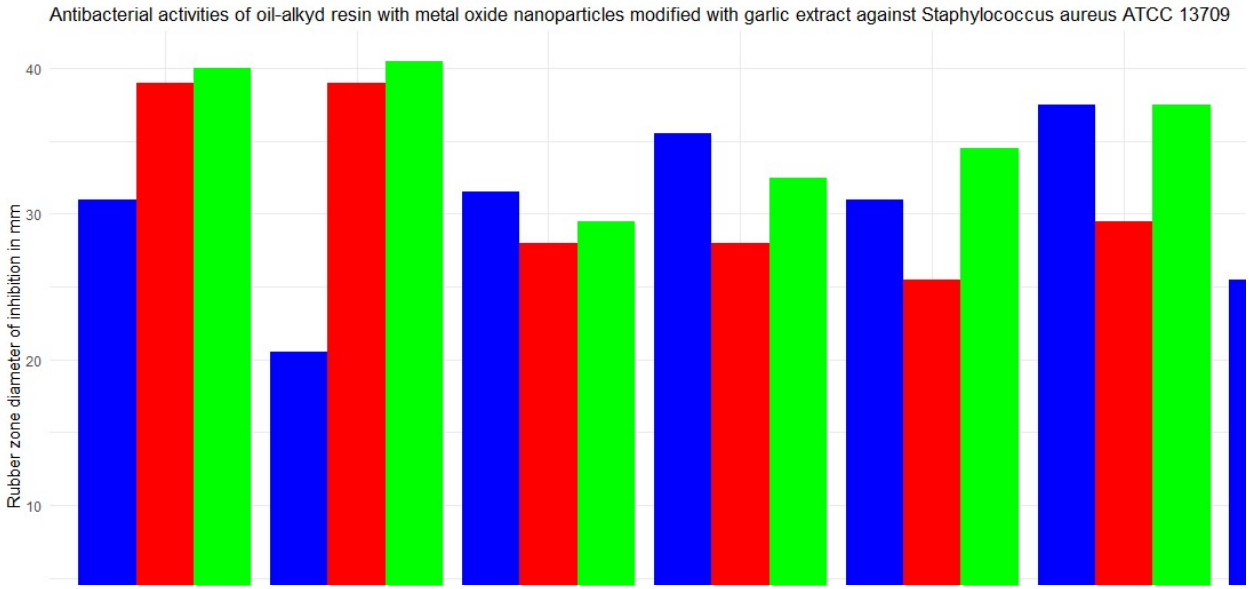

Fig. 10: Antibacterial activities of rubber oil-alkyd resin with metal oxide nanoparticles modified with garlic extract against *E. coli, P. aeruginosa and Staphylococcus aureus*

References

Adeosun, S. O., & Oladipo, O. T. (2014). Synthesis and characterization of alkyd resins from rubber seed oil. *Journal of Chemical Engineering & Process Technology, 5*(3), 1–7. https://doi.org/10.4172/2157-7048.1000207

Aigbodion, A. I., & Pillai, C. K. S. (2000). Preparation, analysis and applications of rubber seed oil and its derivatives in surface coatings. *Progress in Organic Coatings, 38*, 187–192.

Äkräs, L., Vahvaselkä, M., Silvenius, F., Seppälä, J., & Ilvesniemi, H. (2022). A multi-criteria decision-making framework and analysis of vegetable oils to produce bio-based plastics. *Industrial Crops and Products, 188*, 115584.

AOAC International. (2012). *Official methods of analysis of AOAC International* (19th ed.). AOAC International.

Association of Official Analytical Chemists (AOAC). (1990). *Official methods of analysis* (15th ed.). AOAC.

Balouiri, M., Sadiki, M., & Ibnsouda, S. K. (2016). Methods for in vitro evaluating antimicrobial activity: A review. *Journal of Pharmaceutical Analysis, 6*(2), 71–79. https://doi.org/10.1016/j.jpha.2015.11.005

Bamgboye, A. I., & Adejumo, O. I. (2010). Physicochemical properties of roselle seed oil. *Nutrition & Food Science, 40*(2), 186–192.

Bobalek, E. G., & Chiang, C. C. (1964). Synthesis and properties of some alkyds of more than one acid. *Journal of Polymer Science Part A: General Papers, 2*(3), 1105–1114.

Chiplunkar, P. P., and Pratap, A. P. "Utilization of sunflower acid oil for synthesis of alkyd resin", Progress in Organic Coatings, vol. 93, pp. 61-67, 2016.

Chiplunkar, P. P., Shinde, V. V., & Pratap, A. P. (2017). Synthesis and application of palm fatty acid distillate based alkyd resin in liquid detergent. *Journal of Surfactants and Detergents, 20*(1), 137–149.

Dizman, C., & Kaçakgil, E. C. (2023). Alkyd resins produced from bio-based resources for more sustainable and environmentally friendly coating applications. *Turkish Journal of Chemistry, 47*(1), Article 2. https://doi.org/10.55730/1300-0527.3511

Elabor, I., Ikhuoria, E. U., Bakare, I. O., Okieimen, F. E., & Aigbodion, A. I. (2023). Synthesis and characterization of alkyd resins from rubber seed/soybean oil blends. *Nigerian Journal of Technology, 42*(3), 322–329. https://doi.org/10.4314/njt.v42i3.4

Emelike, U. N., & Eke, S. I. (2020). Evaluation of the physicochemical properties of rubber seed oil. *Journal of Agricultural Chemistry and Environment, 15*(1), 58–67. https://doi.org/10.1016/j.jage.2020.04.001

Eze, C. O., & Agomuo, E. O. (2021). Refining effects on the quality of rubber seed oil for biodiesel production. *Energy Reports, 7*, 819–825. https://doi.org/10.1016/j.egyr.2021.01.031

Flores, S., Flores, A., Calderon, C., & Obregon, D. (2019). Synthesis and characterization of sacha inchi (*Plukenetia volubilis* L.) oil-based alkyd resin. *Progress in Organic Coatings, 136*, 105289.

George, K., Reghu, C., & Nehru, C. (2000). By-products and ancillary source of income. In *Natural Rubber Agromanagement and Crop Processing* (pp. 509–520). Rubber Research Institute of India.

Gunstone, F. D., Harwood, J. L., & Pardly, F. B. (1994). *The lipids handbook* (2nd ed.). Chapman & Hall.

Huang, Y., Zhang, W., Xiao, S., & Chen, Y. (2020). Recent advances in antibacterial strategies for multidrug-resistant bacteria: Lessons from nanomaterials. Materials Today Bio, 6, 100056. https://doi.org/10.1016/j.mtbio.2020.100056

Ibrahim, I. S., & Al-Sabagh, A. M. (2020). Characterization of alkyd resins based on vegetable oils and their applications in coatings. *Polymer-Plastics Technology and Engineering, 59*(8), 847–862. https://doi.org/10.1080/03602559.2020.1733300

Ifijen, I. H., Udokpoh, N. U., Onaiwu, G. E., Jonathan, E. M., & Ikhuoria, E. U. (2022). Coating properties of alkyd resin, epoxy resins and polyurethane based nanocomposites: A review. *Momona Ethiopian Journal of Science (MEJS), 14*(1), 1–31.

Ikhuoria, E. U., Aigbodion, A. I., & Okieimen, F. E. (2004). Enhancing the quality of alkyd resins using methyl esters of rubber seed oil. *Tropical Journal of Pharmaceutical Research, 3*, 311–317.

ISO 22196:2011. (2011). *Measurement of antibacterial activity on plastics and other non-porous surfaces*. International Organization for Standardization.

Kalu, K. M., Emmanuel, M., Chinedu, E. K., Akinterinwa, A., Titus, U., Kenneth, R., Haruna, N. A., & Aliyu, B. A. (2023). Extraction, synthesis and characterization of an alkyd resin from *Sesamum indicum* seed oil. *Open Access Library Journal, 10*, e1044.

Kumar, P., & Kumar, V. (2019). Garlic extract-mediated green synthesis of zinc oxide nanoparticles and their antimicrobial activity. *Journal of Nanoparticle Research, 21*(10), 1–12. https://doi.org/10.1007/s11051-019-4634-8

Lligadas, G., Ronda, J. C., Galia, M., & Cadiz, V. (2013). Renewable polymeric materials from vegetable oils: A perspective. *Materials Today, 16*, 337–343.

MacDonald, D., & McKeen, L. (1994). Effect of temperature and catalyst on the synthesis of alkyd resins from rubber seed oil. *Journal of Applied Polymer Science, 54*(6), 833–839. https://doi.org/10.1002/app.1994.070540608

Menkiti, M. C., & Onukwuli, O. D. (2011). Utilization potentials of rubber seed oil for the production of alkyd resins using variable base oil lengths. *Journal of Applied Polymer Science, 121*(3), 1569–1577. https://doi.org/10.1002/app.33750

Mohammadi, N., Ostovar, N., & Granato, D. (2023). *Pyrus glabra* seed oil as a new source of mono and

polyunsaturated fatty acids: Composition, thermal, and FTIR spectroscopic characterization. *LWT, 181*, 114790.

Mustapha, A. O., Ayoku, H. B., & Amao, H. A. (2023a). New alkyd resins from underutilized indigenous seed oils: Synthesis and characterization. *Karbala International Journal of Modern Science, 9*(2). https://doi.org/10.33640/2405-609x.3293

Nekhavhambe, E., Mukaya, H. E., & Nkazi, D. B. (2019). Development of castor oil–based polymers: A review. *Journal of Advanced Manufacturing and Processing, 1*(4), e10030.

Ojo, O. A., & Adeyemi, O. (2020). Physicochemical properties of rubber seed oil and its potential as a biodiesel feedstock. *Energy Reports, 6*, 1–10. https://doi.org/10.1016/j.egyr.2019.11.019

Okieimen, F. E., Pavithran, C., & Bakare, I. O. (2005). Epoxidation and hydroxlation of rubber seed oil: One-pot multi-step reactions. *European Journal of Lipid Science and Technology, 107*(5), 330–336.

Oladipo, I. C., Adebayo-Tayo, B. C., & Olaniran, A. O. (2013). Antimicrobial activity of silver nanoparticles synthesized using *Citrullus lanatus* fruit rind extract. *Journal of Nanotechnology, 2013*, Article 123456. https://doi.org/10.1155/2013/123456

Olaoluwa, O., Adebayo, A., & Adeyemi, T. (2017). Green synthesis of zinc oxide nanoparticles using *Musa paradisiaca* leaf extract and their antibacterial activity. *International Journal of Nanomedicine, 12*, 123–130.

Otabor, G. O., Ifijen, I. H., Mohammed, F. U., Aigbodion, A. I., & Ikhuoria, E. U. (2019). Alkyd resin from rubber seed oil/linseed oil blend: A comparative study of the physiochemical properties. *Heliyon, 5*, e01621. https://doi.org/10.1016/j.heliyon.2019.e01621

Paraskar, P. M., & Kulkarni, R. D. (2021). Synthesis of isostearic acid/dimer fatty acid-based polyesteramide polyol for the development of green polyurethane coatings. *Journal of Polymers and the Environment, 29*(1), 54–70.

Patel, H., & Desai, P. (2020). Rubber seed oil-based alkyd resins for high-performance coatings: A comparative study. *Polymer Engineering and Science, 60*(4), 919–931. https://doi.org/10.1002/pen.25498

Peters, M. A., Alves, C. T., Wang, J., & Onwudili, J. A. (2022). Subcritical water hydrolysis of fresh and waste cooking oils to fatty acids followed by esterification to fatty acid methyl esters: Detailed characterization of feedstocks and products. *ACS Omega, 7*(50), 46870–46883.

Rajendran, A., Subramaniam, S., & Thirumalai, D. (2021). Role of metal oxide heterostructures in photocatalysis: TiO_2/ZnO/CuO nanocomposites for environmental applications. *Journal of Environmental Chemical Engineering, 9*(2), 104678. https://doi.org/10.1016/j.jece.2021.104678

Rani, M., & Singh, S. (2019). Comprehensive analysis of rubber seed oil and its potential use in biodiesel production. *Energy Sources, Part A: Recovery, Utilization, and Environmental Effects, 41*(6), 678–684. https://doi.org/10.1080/15567036.2019.1609073

Rozali, N. L., Azizan, K. A., Singh, R., Syed Jaafar, S. N., Othman, A., Weckwerth, W., & Ramli, U. S. (2023). Fourier transform infrared (FTIR) spectroscopy approach combined with discriminant analysis and prediction model for crude palm oil authentication of different geographical and temporal origins. *Food Control, 146*, 109509.

Satheesh Kumar, M. N., Yaakob, Z., Maimunah, S., Siddaramaiah, S. R. S., & Abdullah, S. R. S. (2010). Synthesis of alkyd resin from non-edible Jatropha seed oil. *Journal of Polymers and the Environment, 18*, 539–544. https://doi.org/10.1007/s10924-010-0188-x

Sati, A., Nandiwdekar, O., Ratnaparkhi, A., Doke, R. B., Pinjari, D. V., Mali, S. N., & Pratap, A. P. (2025). Bio-based alkyd–polyesteramide–polyurethane coatings from castor, neem, and karanja oils with inherent antimicrobial properties for enhanced hygiene. *Coatings, 15*, 370. https://doi.org/10.3390/coatings15040370

Steinerová, D., Kalendová, A., Machotová, J., Knotek, P., Humpolíček, P., Vajdák, J., Slang, S., Krejčová, A., Beneš, L., & Wolff-Fabris, F. (2022). Influence of metal oxide nanoparticles as antimicrobial additives embedded in waterborne coating binders based on self-crosslinked acrylic latex. *Coatings, 12*(10), 1445. https://doi.org/10.3390/coatings12101445

Uzoh, C. F., Obele, M. C., Umennabuife, U. M., & Onukwuli, O. D. (2016). Optimization of the physico-chemical properties of alkyd resin from rubber seed oil by varying polyol composition. *Journal of Applied Polymer Science, 133*(22), 43464. https://doi.org/10.1002/app.43464

Villani, M., Bertoglio, F., Restivo, E., Bruni, G., Iervese, S., Arciola, C. R., Carulli, F., Iannace, S., Bertini, F., & Visai, L. (2020). Polyurethane-based coatings with promising antibacterial properties. *Materials, 13*, 4296.

Wagle, P. G., Tamboli, S. S., & More, A. P. (2021). Peelable coatings: A review. *Progress in Organic Coatings, 150*, 106005.